RLINK: A Realistic Simulation Model of Links in Wireless Sensor Networks

CHEN Hai-ming[1,2], *CUI Li*[1]
(1. Institute of Computing Technology, Chinese Academy of Sciences, Beijing 100190, China;
2. Graduate School of the Chinese Academy of Sciences, Beijing 100039, China)

Abstract: In network simulation, the accuracy of the link model has significant impacts on the credibility of the simulation results. Based on the core feature of links obtained from the recent empirical studies, a realistic link model, named RLINK, was proposed for a more credible simulation of wireless sensor networks (WSNs). *RLINK captured the essential non-isotropic feature of the wireless links in WSNs by modeling three main causes: variance of path loss due to shadowing effect, difference in hardware calibration and radio directionality.* The accuracy of RLINK model was verified by the high agreement of the statistical results obtained from simulations with those obtained from experiments, in terms of cumulative distribution of link asymmetry and arithmetic average of link asymmetry.
Key words: link model; non-isotropic radio connectivity; shadowing effect; wireless sensor network

RLINK: 一种真实的无线传感器网络链路仿真模型

陈海明[1,2]，崔 莉[1]
（1.中国科学院计算技术研究所，北京 100190；2.中国科学院研究生院，北京 100039）

摘 要：在网络仿真中，链路模型的精确性对仿真结果的真实性有着重要影响。基于在无线传感器网络实验中观察到的链路的核心特殊性质——**不等向连通性**，提出了一个真实的链路仿真模型 RLINK.**通过对不等向连通性的三个因素进行分析建模，即由遮蔽效应引起的路径衰减的差异、节点硬件的校准差异和天线的方向性差异，该模型实现了无线传感器网络链路的精确模拟。**以链路不对称性的累积分布和算数平均值为指标，对比实验和仿真中获得的有关链路特性的统计数据，两者的一致性验证了 RLINK 的精确性。
关键词：链路模型；不等向连通性；遮蔽效应；无线传感器网络
中图分类号：TP393 **文献标识码：**A **文章编号：**1004-731X (2010) 12-2967-06

Introduction

The accuracy of the link model has significant impacts on the credibility of the simulation results, since the node connectivity determines the behaviors of upper layer protocols. Due to the discrepancy between the commonly used link models, e.g. disc model, and the real link features, researchers begin realizing that the simulation results are sometimes inconsistent with the network performance in practice, especially for the wireless networks. So some improved link models were proposed for the wireless networks.

Most of the currently proposed models are based on the following propagation model, namely free-space, two-ray ground, shadowing and ricean. Those models have been implemented in NS2, and are widely used in the simulation of 801.11 based wireless networks. However, we think that it is unreasonable to apply those models directly to the wireless sensor networks, since recent empirical studies on the link characteristics reveal some unique features for the wireless sensor networks.

In this paper, we first present some statistical results on the link characteristics of wireless sensor networks obtained from the recent empirical studies. Based on the statistical results, then we propose a realistic simulation model, named RLINK, for wireless sensor networks. RLINK captures the core feature of links in wireless sensor networks, i.e., non-isotropic radio connectivity, by modeling three main causes: variance of path loss due to shadowing effect, difference in hardware calibration and radio directionality.

The contributions of the paper are embodied in the following aspects:

1) Based on the featuring phenomena observed in recent empirical studies, we explain why the non-isotropic radio connectivity is the core feature of links in wireless sensor networks.

2) We analyze the main causes leading to the non-isotropic radio connectivity, i.e., variance of path loss due to shadowing effect, difference in hardware calibration and radio directionality.

3) Taking these causes into account, we propose a realistic simulation model of links in wireless sensor networks. The

Received: 2008-12-31 **Revised:** 2009-03-08
Foundation item: National Basic Research Program of China (973 Program) under Grant No. 2006CB303001, National High Technology Research and Development Program of China (863 Program) under Grant No. 2007AA01Z2A9, CAS Knowledge Innovation Program under Grant No. KGCX2-YW-110-3, CAS- Croucher Funding Scheme for Joint Laboratories and Key External Cooperation Program of the Chinese Academy of Sciences under Grant No. GJHZ200819.
Biography: Haiming Chen (1981-), Male, Ph.D, interested in network protocol design and performance evaluation; **Li Cui** (1962-), Female, Professor, Ph.D supervisor, interested in sensing technology and sensor networks.

proposed model is implemented in a network simulator, and its accuracy is verified by the high agreement of the statistical results obtained from simulations with those obtained from experiments.

1 Link Characteristics

1.1 Actual link characteristics observed in empirical studies

Table 1 gives an overview on the recent empirical studies on the link characteristics of wireless sensor networks. Those studies were conducted in different environments with different experimental settings in terms of mote types, RF modules, transmitting powers. From the statistical results published in [1-4], we conclude that following three featuring phenomena were observed in all those studies.

1) *Non-isotropic radio connectivity:* which means neighbors having the same distance to the transmitting node may have different probabilities of receiving packets successfully. In other words, the contour map of the packet reception ratio with respect to distance was not a set of concentric circles.

2) *Gray area:* in which the packet delivery probability varies with no clear relation with distance. In other words, the packet reception ratio in this area is a random variable about the distance.

3) *Asymmetric links:* which means links in the forward and reverse directions may have different reception ratios.

To verify the existence of the above phenomena, we also conducted some indoor experiments with the same topology described in [3], and gathered some statistics in terms of packet delivery ratio. Fig. 1(a) shows a corner of the experimental environment. We tuned the output power of the nodes (MICA2 series) to a low level (-16 dBm), so the reliable transmission range is about 8 meters. Fig. 1(b) shows the existence of non-isotropic radio connectivity, and Fig. 1(c) gives an illustration of the gray area.

The above three phenomena provide a guideline for developing a realistic simulation model of links. Now a question arises: *should we take all these phenomena simultaneously into consideration when developing the link model*? To answer the question, we attempt to clarify the relationships among these phenomena and capture the core feature.

1.2 Non-isotropic radio connectivity: the core feature of links

Firstly, we investigate the relationship between the gray area and non-isotropic radio connectivity. Each dot in Fig. 1(c) represents the packet reception ratio for the link of distance d. The links of distance d can be independent or dependent. For independent links, they have different sources and ends. For dependent links, they share the same source with different ends.

Considering Fig. 1(c) as the scatter plot of the packet reception ratio of the *dependent* links, the dots scattered in the line of $x = d$ can be viewed as the packet reception ratios of neighbors, which are d meters away from the transmitter. So the link characteristics inside or outside the gray area presented in Fig. 1(c) can also be explained in following ways. (i) When

Table 1. recent empirical studies on the link characteristics of wireless sensor networks

Ref. work / Settings	[1]	[2]	[3]		[4]
Mote	Rene	Mica	Mica	Mica2	EYES
RF Module	TR1000	TR1000	TR1000	CC1000	TR1001
Frequency (MHz)	916	916	916	433	868
Modulation	OOK	ASK	ASK	FSK	ASK
Data rate (kbps)	< 10	< 20	13.3	19.2	115
Encoding	SECDED	SECDED & Manchester & 4B5B	SECDED	Manchester	4B8B
TX Power (dBm)	-40~-24	Default	10~0	-15~5	Fixed
Environments	Open parking structure	Parking lot State park Hockey	State park School courtyard Ceiling of the lab		Hockey pitch Tennis court Corridor

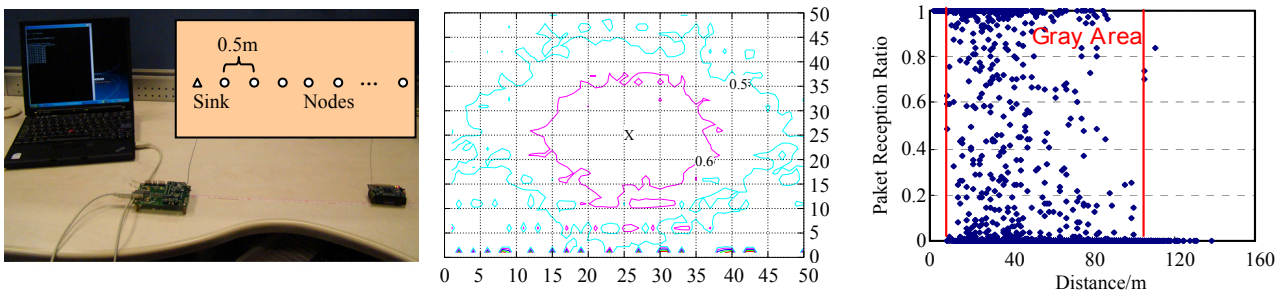

(a) Experimental environment (b) Non-isotropic radio connectivity (c) Gray area

Fig. 1 Experimental environment and results observed in our experiments

neighbors are located near the transmitter, they have similarly high probabilities to receive packets successfully; (ii) as they are located farther away from the transmitter, the packet reception ratio becomes diverse. These two observations are just what the Fig. 1(b) shows: (i) contours close to the transmitter are resembling circles; (ii) they become irregular as the radius increases.

From the above analysis, we can conclude that the prevalence of gray area can be explained by the non-isotropic radio connectivity.

Secondly, we examine the relationship between the link asymmetry and non-isotropic radio connectivity. Fig. 2(a) shows the packet transmission between two nodes with identical non-isotropic connectivity, supposing curves around the nodes are the contours of 80% packet reception ratio. From this figure, we can see that the link connectivity from B to A is about 0.8, while it is less than 0.8 from A to B. So the link between A and B is an instance of asymmetric links caused by the non-isotropic radio connectivity.

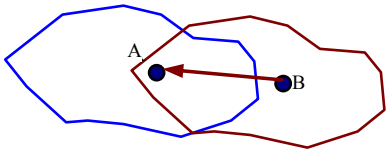

(a) A asymmetric link caused by the non-isotropic radio connectivity

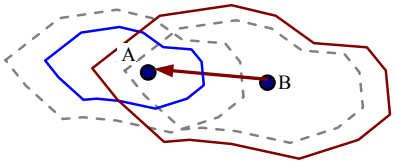

(b) More link asymmetry caused by the difference in output power

Fig. 2 Illustration of link asymmetry in wireless sensor networks

Difference in hardware calibration and energy levels between nodes can lead to different output powers, which can cause the nodes to have different patterns of connectivity. As Fig. 2(b) shows, supposing node B has a larger output power than node A, the resulting different connectivity pattern can increase the difference of packet reception ratio, and make the link between A and B more asymmetric.

According to the above analysis, we can conclude that *the non-isotropic radio connectivity can be the essential reason for asymmetric links*, while the difference in hardware calibration and energy levels between nodes can make the link more asymmetric.

In short, through analyzing the relationships among non-isotropic radio connectivity, gray area and asymmetric links, we are confirmed that *non-isotropic radio connectivity* is the core feature of links in wireless sensor networks, which is the unique characteristic supposed to be taken into consideration when developing a realistic simulation model of links.

2 Causes of the Non-isotropic Radio Connectivity

2.1 Log-normal shadowing path loss

It is well known that radio signal suffers from distance attenuation when propagating from the source to its neighbors. Path loss is such a metric describing the channel attenuation at a specific location. To the best of our knowledge, the most commonly used path loss models include free space model and two-ray model. Both assume circular propagation coverage area. However, the prevalence of non-isotropic radio connectivity proves that these two models do not hold true for the wireless sensor networks.

The non-isotropic radio connectivity can be primarily attributed to the shadowing effect. Due to the shadowing effect, the path losses of nodes having the same distance to the transmitter can vary with nodes' location. Lots of measurements have shown that the variation of the large-scale path loss is often log-normally distributed about the mean path loss [5].

$$\overline{PL}(d)[\mathrm{dB}] = PL(d_0)[\mathrm{dB}] + 10 \cdot n \cdot \log_{10}(d / d_0) \quad (1)$$

$$PL(d)[\mathrm{dB}] = \overline{PL}(d)[\mathrm{dB}] + X_\sigma[\mathrm{dB}] \quad (2)$$

where $\overline{PL}(d)$ is the mean path loss in dB, $PL(d_0)$ is the free-space path loss at a close-in reference distance d_0, n is the path loss exponent, and X_σ is a zero-mean log-normally distributed (normal in dB) random variable with standard deviation σ in dB. n and σ are related with propagation environment.

2.2 Difference in hardware calibration

All the previous empirical studies presented in Section 1.1 show that even with the same hardware settings, actual output power and receiver sensitivity can vary for different nodes. This inherited difference in hardware calibration can be another reason contributing to the different connectivity probabilities for the nodes having the same distance to the transmitter.

As for the impact of difference in output power on the connectivity pattern, we have explained in Section 1.2 (see fig. 2). Here we give an example to clearly explain how the difference in receiver sensitivity leads to the non-isotropic radio connectivity.

As Fig. 3 shows, Node I is far away from Node R1, R2 and R3, signal propagating to them has been attenuated to a very low power, say -102 dBm. R1, R2 and R3 have different receive sensitivities, say -100 dBm for R1, -102 dBm for R2 and -101 dBm for R3. So only can R2 sense the radio propagated from Node I, and switch its state to receiving. Supposing Node S (if it fails to back off properly) starts to transmit a packet exactly at that time, R1, R2 and R3 are all supposed to receive the signal with a high probability. However, since R2 receives signal from node I, it will regard the signal from Node S as interference, and ignore the packet from Node S. So R2 have totally different packet reception ratio from R1

and R3, due to its slightly more sensitive receiving capability.

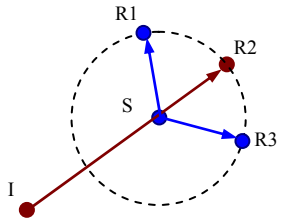

Fig. 3 Non-isotropic radio connectivity caused by difference in receiver sensitivity between nodes. The dashed line indicates that R1, R2 and R3 have the same distance to S, rather than have the same connectivity probability to S.

2.3 Radio directionality

Nodes used in current experimental measurements are commonly equipped with omni- directional antenna, which is supposed to radiate power equally in all directions. However, the output power often varies with direction in reality. This phenomenon can be primarily attributed to the small variance of antenna gain in different directions. For the same reason, the directionality in receiver sensitivity is observed in the empirical studies.

In short, the variance of path loss due to shadowing effect, along with difference in hardware calibration and radio directionality, leads to the non-isotropic radio connectivity in wireless sensor networks.

3 Design of the RLINK Model

The link model consists of two components, namely radio propagation component and signal reception component. So we design the RLINK model in following two steps.

1) Design a radio propagation component to determine the strength of attenuated signal when it is received by the neighbors. The three analytical results about the causes of the non-isotropic radio connectivity are the principal guidelines to design a radio propagation component in a realistic way.

2) Based on the received signal strength computed by radio propagation model, and taking the interference from simultaneous transmissions into consideration, we develop a SINR- BER (Signal to Interference plus Noise Ratio-Bit Error Rate) based signal reception component.

3.1 Non-isotropic radio propagation

According to the cause 2, even if the nodes are tuned to send packet in the same power, the actual output power can be varied for different nodes. Computing from our measurements by linear regression in a minimum mean square error (MMSE) sense, we find that the output power of the nodes can be well modeled by a normally distributed variable with mean P_t and standard deviation V_{op}. P_t is the nominal output power, which is 0 dBm by default in most cases. V_{op} is the root-mean-square deviation of the output power from P_t.

Further more, according to the cause 3, we adjust the output power of different directions by a small variation of the antenna gain. The actual output power of the transmitter is formulated by the following equation.

$$P_t^{'} = P_t \cdot (1 + r \cdot V_{op} / P_t) + G_t \cdot D(x) \tag{3}$$

r is a random variable following the standard normal distribution, so $P_t \cdot (1 + r \cdot V_{op} / P_t)$ is normally distributed with mean P_t and standard deviation $V_{op.}$ G_t is the nominal antenna gain of the transmitter in dB, and $D(x)$ is a function which returns a coefficient to adjust the antenna gain in the direction of x degree. The function $D(x)$, which is defined in Equation (4), is used to generate continuous variation of the antenna gain in the direction of radio propagation.

$$D(x) = \begin{cases} 1 + r \cdot V_{ant} / G_{t.} & x \in N \\ D(s) + (x - s) \cdot [D(t) - D(s)], & x \notin N \end{cases} \tag{4}$$

where $0 \le x < 360$, $s = \lfloor x \rfloor$, $t = \lceil x \rceil \mod 360$, and N is the set of integers. V_{ant} is the standard deviation of antenna gain per unit degree change, and r is a standard-normally distributed random variable.

For the receiver, according to the cause 1 and cause 3, the power of the received signal is formulated by the following equation.

$$P_r^{'} = P_t^{'} - PL + G_r \cdot D(x) \tag{5}$$

where PL is the path loss formulated by the equation (2), and G_r is the nominal antenna gain of the receiver and $D(x)$ is defined in the equation (4).

It is based on the receiving sensitivity to determine whether the propagated signal of strength $P_r^{'}$ can be sensed by the receiver. According to the cause 2, the actual receiving sensitivity can be varied for different nodes. Computing from our measurements by linear regression in a minimum mean square error (MMSE) sense, we find that the receiving sensitivity can also be well modeled by a normally distributed variable with mean S_r and standard deviation V_{rs}. So the actual receiving sensitivity of each node is formulated by the following equation.

$$S_r^{'} = S_r \cdot (1 + r \cdot V_{rs} / S_r) \tag{6}$$

S_r is the nominal receiving sensitivity, and V_{rs} is the root-mean-square deviation of the receiving sensitivity from S_r. r is a random variable following the standard normal distribution.

The nominal output power P_t, the nominal receiving sensitivity S_r, the nominal antenna gain G_t and G_r are all provided as the basic parameters of radio frequency modules (RFMs). For example, S_r is about -103 dBm for CC1000 when it is set to work with FSK modulation scheme and 19.2 Kbps data rate.

It is worth noting that in Equation (3), (4) and (6), $P_t^{'}$, $D(x)$ and $S_r^{'}$ are each formulated by a normally- distributed variable with corresponding mean and standard deviation, but are all

generated with one standard-normally distributed variable r by expressing those random variables in a changed form. Concretely, if a random variable is normally-distributed with u mean and v standard deviation, it can also be expressed by $u\cdot(1+r\cdot v/u)$. Through this transformation, we can implement all the above models using one random number generator.

3.2 SINR-BER based reception model

It is well known that the bit error rate (BER, p_b) can be estimated from SINR (Signal to Interference plus Noise Ratio), which is defined as follows:

$$\gamma = \frac{P_r'}{P_i + P_n} \tag{7}$$

where P_r' is the power of the received signal, P_i is a accumulation of the interferences from all the simultaneous transmissions, and P_n is the noise.

Although BER solely depends on SINR, the relationship between the SINR and BER is a function of modulation scheme. Fig. 4 gives a comparative view on the relationship between SINR and BER for these modulation schemes, namely OOK, FSK and DPSK, which are commonly used in wireless sensor networks.

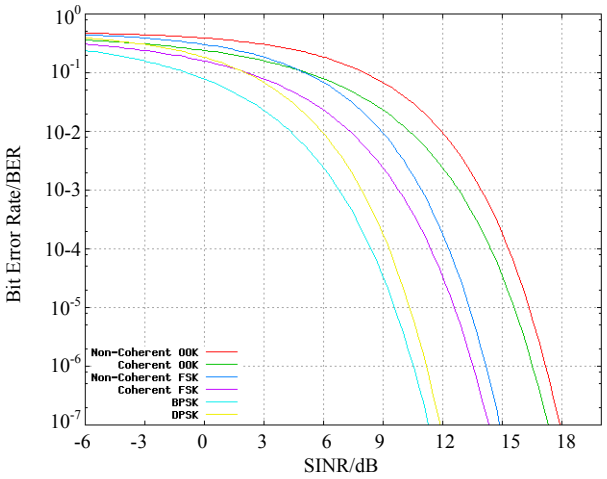

Fig. 4 Relationship between SINR and BER for different modulation schemes

When the BER is p_b, the probability of successfully receiving a packet is:

$$p = (1\text{-}p_b)^{8f} \tag{8}$$

where f is total length of the packet in byte, including the preamble/start symbol overhead, packet header overhead and payload.

In short, the RLINK model works in following steps. When a node transmits a packet, it will compute the output power and the received power of all its neighbors, according to the equation (3) and (5). Then, each neighbor judge whether the received power is above its receiving sensitivity, according to the equation (6). At last, the neighbors who can sense the signal determine the probability of packet reception probability, according to the equation (7) and (8).

4 Accuracy Verification of the RLINK Model

To verify the accuracy of the RLINK model, we implemented it in the EasiSim simulator [7]. We set up a simulation scenario with the same topology described in Section 1.1 (see fig. 1), and examine the link characteristics in the indoor environments. Path loss exponent and standard deviation (n,δ) for the indoor environment is (2.76, 12.9).

Parameters of the nodes are set according to the statistics obtained from the experimental measurements. Details of the parameters and their settings are listed in Table 2. We collect following two statistics in simulations.

1) *Number of link pairs:* a link pair is referred to as the links of the forward and reversed directions between a pair of nodes.

2) *Link asymmetry:* defined as the packet reception difference of a link pair.

Table 2. Parameters of the nodes in the simulation

Notation	Parameter	Value
P_t	Nominal output power	0 dBm
V_{op}	Standard deviation of output power	-10 dBm
S_r	Nominal receiving sensitivity	-103 dBm
V_{rs}	Standard deviation of receive sensitivity	-110 dBm
G_t, G_r	Nominal antenna gain	0 dBi
V_{ant}	Standard deviation of antenna gain	-10 dBi

2) *Cumulative distribution of link asymmetry*: defined as $P(D_i) = N_{D_i} / n$, where N_{D_i} is the number of link pairs with link asymmetry up to D_i, ($0 \le D_i \le 1$), n is the number of link pairs collected in simulation.

Table 3 shows the number of link pairs and the average of link asymmetry obtained from experiments and simulations. Fig. 5 shows the cumulative distribution of link asymmetry of the links obtained from experiments and simulations.

Table 3. Number of link pairs and average of link asymmetry collected from experiments and simulations

	Number of link pairs	Average of link asymmetry
Experiment	9247	0.251
Simulation	9255	0.263

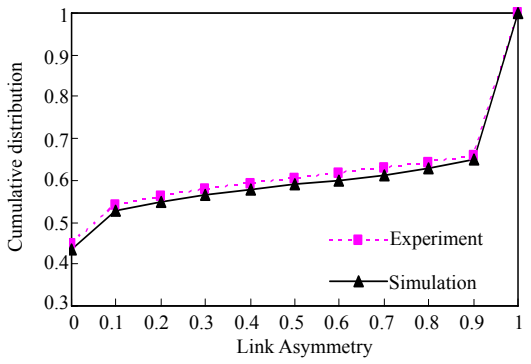

Fig. 5 Cumulative distribution of link asymmetry

The accuracy of the implemented link model is verified by comparing the statistics obtained from simulation with that from empirical studies in terms of following metrics.

1) *Arithmetic average of link asymmetry:* defined as $\overline{D} = \frac{1}{n}\sum_{i=1}^{n} D_i$, where n is the number of link pairs collected in simulation, and D_i is the link asymmetry of each link pair.

Using the experimental results as the benchmark, we can see that links implemented by our model almost have the same characteristics with that collected in experiments. The small difference in the two metrics can be mainly attributed to the unavoidable errors of the parameters modeling the environment and the nodes.

5 Related Work

Considering the non-isotropic property of radio connectivity in wireless sensor networks, He *et al* [7] proposed a simple DOI (Degree of Irregularity) model. Woo *et al* [8] proposed a method to associate a normally distributed random number with each directed node pair as the non-isotropic connectivity probability. Zuniga *et al* [9] designed a tool to generate a matrix with connectivity probability for all the links the network, based on the log-normal shadowing path loss model. Cerpa *et al* [10] proposed a new link generator based on the non-parametric statistical models. Zhou *et al* [11] proposed a RIM (Radio Irregularity Model) model to simulate the irregular received signal strength.

In short, currently the proposed link models are still idealized. They either associate a random value (between 0 and 1) with each pair of nodes as the connectivity probability, or adjust the received signal strength by simply multiplying the path loss (free space or two-ray model) by a random coefficient. On the contrary, the RLINK model proposed in this paper is designed based on the deep analysis of the causes of the non-isotropic radio connectivity in wireless sensor networks. Besides that, the RLINK model can be easily adapted to simulate links in wireless sensor networks with different node settings, by changing the parameters listed in Table 2.

6 Conclusion

In this paper, we first present some statistical results on the link characteristics of wireless sensor networks obtained from some recent empirical studies. Based on these results, we derive the *non-isotropic radio connectivity* as the core feature of links in wireless sensor networks, from deep analysis of the relationships among the three link characteristics, namely non-isotropic radio connectivity, gray area and asymmetric links. To model the core feature of the links, we then analyze the main causes leading to the non-isotropic radio connectivity, namely variance of path loss due to shadowing effect, difference in hardware calibration and radio directionality. Taking these causes into account we designed a realistic link model, named RLINK. Besides that, we implement the RLINK model in a network simulator, and verified its accuracy by the high consistence of the statistical results collected from simulations and measurements, in terms of cumulative distribution of link asymmetry and arithmetic average of link asymmetry.

Because in this paper we concentrate our efforts on the spatial characteristics of links in wireless sensor networks, the noise floor is assumed invariant with time. We will improve the accuracy of RLINK model by taking the temporal dynamics [12] of noise into consideration in our future work.

Reference:

[1] D Ganesan. An Empirical Study of Epidemic Algorithms in Large Scale Multihop Wireless Networks [R]. California, CA, USA: UCB, Mar. 2002.

[2] J Zhao, R Govindan. Understanding Packet Delivery Performance in Dense Wireless Sensor Networks [C]// Proceedings of Sensys'03. New York, NY, USA, 2003: 1-13.

[3] A Cerpa, N Busek, D Estrin. SCALE: A Tool for Simple connectivity Assessment in Lossy Environments [R]. Los Angeles, USA: CENS, University of California, Sep. 2003.

[4] N Reijers, G Halkes, K Langendoen. Link Layer Measurements in Sensor Networks [C]// Proceedings of MASS'04. Washington, DC, USA, 2004: 224-234.

[5] T S Rappapport. Wireless Communications: Principles and Practice (2nd Edition) [M]. USA: Prentice Hall, 2002.

[6] T He, C Huang, B M Blum, J A Stankovic, T. Abdelzaher. Range-free Localization Schemes for Large Scale Sensor Networks [C]// Proceedings of MobiCom'03. New York, NY, USA, 2003: 81-95.

[7] H-M Chen, L Cui, H Zhu, C-C Huang. EasiSim: A Scalable Simulation Platform for Wireless sensor networks [C]// Proceedings of IEEE CAMAD'08. Washington, DC, USA, 2008: 793-800.

[8] A Woo, T Tong, D Culler. Taming the Underlying Challenges of Reliable Multihop Routing in Sensor Networks [C]// Proceedings of Sensys'03. New York, NY, USA, 2003: 14-27.

[9] M Zuniga, B Krishnamachari. Analyzing the Transitional Region in Low Power Wireless Links [C]// Proceedings of SECON'04. Washington, DC, USA, 2004: 517-526.

[10] A Cerpa, J Wong, L Kuang, M Potkonjak, D Estrin. Statistical Model of Lossy Links in Wireless Sensor Networks [C]// Proceedings of IPSN'05. New York, NY, USA, 2005: 81-88.

[11] G Zhou, T He, S Krishnamurthy, J A Stankovic. Impact of Radio Irregularity on Wireless Sensor Networks [C]// Proceedings of MobiSys'04. New York, NY, USA, 2004: 125-138.

[12] H Lee, A Cerpa, P Levis. Improving Wireless Simulation through Noise Modeling [C]// Proceedings of IPSN'07. New York, NY, USA, 2007: 21-30.